Very Fast Tunneling in the Early Stage of Reaction Dynamics

Hiroshi Ushiyama* and Kazuo Takatsuka†

Department of Basic Science, Graduate School of Arts and Sciences, University of Tokyo, Komaba, 153-8902, Tokyo, Japan

Received: April 23, 2005; In Final Form: October 31, 2005

The difference between quantum and classical survival probabilities for molecular dissociation dynamics in the time domain, which arises mainly from quantum mechanical tunneling, has interesting characteristics that are not noticed through the counterpart in energy domain. It is shown that the early stage undergoes a fast tunneling, while the later stage is characterized with a long-lasting slow tunneling. The mechanism of this behavior is analyzed in terms of a quasi-semiclassical theory featuring the geometrical distribution of the so-called tunneling points. In particular, the role of dynamical tunneling is discussed as a phenomenon that typifies the time dependence of tunneling dynamics. It is predicted that these tunneling characteristics will be reflected in the isotope effect and should be experimentally observable.

I. Introduction

The decaying, escaping, or dissociating process from a prepared state in a potential basin or compound state like the Feshbach resonance is fundamentally important in the dynamics of molecules. The core excited resonance in electron scattering and autoionization state are typical examples of such a decaying state in electron dynamics. On the other hand, rearrangement, dissociation, and structural isomerization of molecules caused by laser excitation are critical processes in modern reaction dynamics. The RRKM (Rice−Ramsperger−Kassel−Marcus) theory is actually a statistical method to evaluate the rate of thermal molecular dissociation, which is also one of the typical decaying states.

In the study of molecular dissociation on a single potential surface, it is crucial to distinguish the decays above and below a potential barrier. The mechanism of decay above the potential barrier has been extensively studied already. For just an example, Agung and Takatsuka have recently found that a quantum effect arising from the so-called periodic orbits suppresses the exponential decay.[1] With an energy below a barrier height, only the quantum mechanical tunneling can drive a decay. Proton transfer is among the most typical chemical situations we think of as an example of tunneling. In fact, the motivation of the present study originated from a couple of case studies on intramolecular proton transfer dynamics in 5-methyltropolone[2] and dichlorotrpolone,[3] and intermolecular double proton transfer in formic acid dimer,[4] and so on. The majority of experimental and theoretical studies on tunneling so far performed[5,6] have placed their focus on static quantities such as tunnel splitting, that is, the dynamics in the energy domain. However, the current progress of ultrafast dynamics[8−12] readily leads us to project that the direct measurement of tunneling in such subtle scales of energy and time will become widely feasible in the near future. Assuming that this will be the case, we report here our theoretical study on the prominent characteristics of the tunneling in the time domain, which will not necessarily be realized by measurements in the energy domain. Here, it is shown with the quantum wave packet approach that the tunneling has an extremely strong time dependence: very fast tunneling in the early stage and slow and long-standing tunneling decay in the later process. The former process seems to be rather counterintuitive. Besides, we show numerically that this strong time dependence can be observed clearly in an isotope effect.

Recently, Wilkinson et al. have shown an experimental example of nonexponential decay in quantum tunneling.[13] They have observed a decay process of an ultracold sodium atom out of an accelerating periodic optical potential created by a standing wave of light. Their conclusion is that the tunneling in the early stage is faster, which makes a significant deviation from the exponential profile. In our theoretical study of the tunneling dynamics of proton transfer, we have noticed a similar phenomenon (very fast tunneling in the early stage). Although the physical situation of our reaction system and that of Wilkinson et al. are totally different, we have realized that there is a physical mechanism that accelerates the tunneling in the early stage. To explain this mechanism, we apply our developed time-dependent quasi-semiclassical trajectory method (TDQSCT)[14] that is based on a semiclassical theory of nonclassical paths.[15−19] After confirming that the TDQSCT reproduces the quantum decay probability well, we analyze the time dependence of the tunneling rate in terms of the number and the geometrical locations of the tunneling points, from which the semiclassical tunneling paths emanate to leave the potential basin where they were initially prepared. We ascribe the fast tunneling in the early stage to the fact that the number and the location of the tunneling points in the early stage are more favorable for accomplishing tunneling dynamics than in the later stage. We also show that such time-dependent characteristics in tunneling dynamics can be clearly observed in the deuteron substitution of proton.

This paper is organized as follows. In section II, we set up our tunneling problem and briefly outline the methods we use. In section III, we show and analyze the numerical results of the quantum mechaical tunneling. Section IV concludes the present paper with some remarks.

II. Tunneling Dynamics in Time Domain with Quantum, Quasi-Semiclassical, and "Classical" Methods

A. Quantum Wave Packet Propagation. We study the following tunneling dynamics on a 2-dimensional double well

* Electronic address: ushiyama@mns2.c.u-tokyo.ac.jp.
† Electronic address: kaztak@mns2.c.u-tokyo.ac.jp.

10.1021/jp0521205 CCC: $30.25
Published on Web 12/06/2005

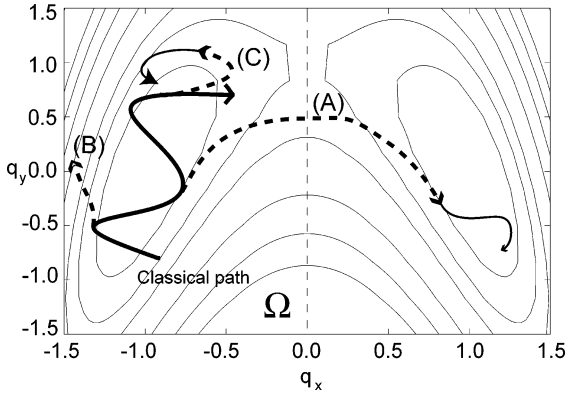

Figure 1. The potetial surface and a schematic representation of a classical trajectory and three kinds of tunneling paths denoted as (A), (B), and (C) corresponding to the classification shown in section II.B.3. The left half of the entire space is denoted as Ω, from which a quantum wave packet escapes. An optical potential is set at $q_x = 0.5$ (not shown).

potential that is intended to model a proton transfer system. The Hamiltonian used here is

$$H(q_x, q_y) = \frac{1}{2m}(\hat{p}_x^2 + \hat{p}_y^2) + 0.125\{(q_x{}^2 - 1)^2 + [q_y + \gamma(q_x{}^2 - 1)]^2\} \quad (1)$$

We set $m = 1$ and $\hbar = 0.1$. The skew parameter is chosen to be $\gamma = 1.0$, which results in a potential form as in Figure 1. This potential supports four bound states below the potential barrier 0.125. We integrate the time-dependent Schrödinger equation with an initial wave packet $\Phi(\vec{q}, t = 0)$ of the following standard form

$$\Phi(\vec{q}, 0) = \left(\frac{2}{\pi\hbar}\right)^{1/2} \exp\left[-\frac{1}{\hbar}(\vec{q} - \vec{q}_c)^2 + \frac{i}{\hbar}\vec{p}_c \cdot (\vec{q} - \vec{q}_c)\right] \quad (2)$$

where $\vec{q} = (q_x, q_y)$. $\vec{q}_c$ and $\vec{p}_c$ are two-dimensional vectors representing the initial position and associated momentum, respectively, at the center of the wave packet. The energy of this type of wave packet is often characterized in terms of E_{center}, which is the sum of the potential energy at $\vec{q}_c$ and the classical kinetic energy arising from $\vec{p}_c$. The survival probability for this packet to remain in a potential basin resisting the tunneling is considered. The center of an initial wave packet is put on $\vec{q}_c = (-1, 0)$ and $\vec{p}_c = (0.2, 0.283)$, resulting in $E_{center} = 0.06$, which is considerably lower than the potential barrier. However, because of the rather sharp Gaussian shape, the energy expectation value $\langle\Phi|H|\Phi\rangle$ results in 0.1886, which is higher than the barrier height by 0.0636. In this study, the dynamics is terminated just after proton transfer is accomplished by placing an absorption potential (artificial optical potential) of the form $V_{opt}(q_x) = 0.5i(q_x - 0.5)$ only in the region $q_x \geq 0.5$, lest the wave packet should come back to the original potential basin through another tunneling or recrossing. To calculate the survival probability, we define an area Ω in which the norm of the wave packet is to be calculated. It is the left half of the space of Figure 1, the boundary of which is set at $q_x = 0$.

The quantum propagation of a wave packet is achieved with the FFT[20] and symplectic integrator method,[21,22] both of which are well-established.

B. Quasi-Semiclassical Method. To analyze the above calculated quantum dynamics, we apply a quasi-semiclassical theory based on the generalized classical paths (nonclassical paths). To be self-contained as much as possible, we briefly review the outline of the theory. The reader may skip to subsection II.C.

1. Multidimensional Tunneling Paths. We try to find a systematic class of nonclassical solutions in the Hamilton−Jacobi equation

$$-\frac{\partial S}{\partial t} = \frac{1}{2}\sum_k \left(\frac{\partial S}{\partial q_k}\right)^2 + V(q) \quad (3)$$

that would be used to describe quantum mechanical tunneling in the Feynman path integrals or semiclassical theories. To find them in the real-valued configuration space q, we start from a little modified Hamilton−Jacobi equation

$$-\frac{\partial S_{cl}}{\partial t} = \frac{1}{2}\sum_k \sigma_k \left(\frac{\partial S_{cl}}{\partial q_k}\right)^2 + V(q) \quad (4)$$

where the constant assigned to each dimension σ_k, called the parity of motion, can take only positive or negative unity. Equation 4 with $\sigma_k = 1$ for all k is nothing but the original Hamilton−Jacobi equation, but otherwise, it gives different solutions. Equation 4 is related to the modified Hamiltonian

$$H(\sigma) = \frac{1}{2}\sum_k \sigma_k \bar{p}_k^2 + V(q) \quad (5)$$

where $\bar{p}_k$ is a quasi-momentum, which is real-valued. By writing

$$\bar{p}_k = \frac{1}{\sigma_k}\frac{\partial S_{cl}}{\partial q_k} \quad (6)$$

one can readily construct a solution of eq 4 as

$$S_{cl}(q, t) = \int \sum_k \sigma_k \bar{p}_k \, dq_k - H(q, \bar{p}) \, dt \quad (7)$$

which is to be integrated along a trajectory that is generated by the modified Hamiltonian, eq 5. Except for the trivial case of $\sigma_k = 1$ for all k, S_{cl} does not satisfy the original Hamilton−Jacobi equation, eq 3. More explicitly, the path $(q, \bar{p})$ in phase space can be generated in terms of the associated canonical equations of motion

$$\frac{d}{dt}(\sigma_k \bar{p}_k) = -\frac{\partial H(\sigma)}{\partial q_k} \text{ and } \frac{dq_k}{dt} = \frac{\partial H(\sigma)}{\partial(\sigma_k \bar{p}_k)} \quad (8)$$

Notice that, if all the parities are negative, the resultant paths become equivalent to the instanton paths.

The derivative of S_{cl} generates a natural vector field on configuration space, that is

$$\sigma\bar{p}(q) = (\sigma_1\bar{p}_1(q), \sigma_2\bar{p}_2(q), \sigma_3\bar{p}_3(q), \cdots) \quad (9)$$

Making use of this, we now define a new vector field by

$$\sqrt{\sigma}p(q) = [\sqrt{\sigma_1}\bar{p}_1(q), \sqrt{\sigma_2}\bar{p}_2(q), \sqrt{\sigma_3}\bar{p}_3(q), \cdots] \quad (10)$$

So far, we do not have to know a generating function that gives this field. Define the individual component on this vector field at (q, t) as

$$\frac{\partial S_{HJ}(q, t)}{\partial q_k} \equiv \sqrt{\sigma_k}\bar{p}_k \quad (11)$$

It is obvious that $\partial S_{HJ}(q, t)/\partial q_k$ formally satisfies

$$\frac{1}{2}\sum_k \left[\frac{\partial S_{HJ}(q, t)}{\partial q_k}\right]^2 + V(q) = H(\sigma) \tag{12}$$

So far, only the differential vector field is defined, but the value of $S_{HJ}(q, t)$ is not. Although an infinite number of functions can be made up whose derivative give the same vector field, one may specify its value by integrating eq 11 along the vector field, that is, a path $(q, \bar{p})$ of eq 8 such that

$$S_{HJ}(q, t) = \int \sum_k \sqrt{\sigma_k}\, \bar{p}_k(q)\, \mathrm{d}q_k - H(\sigma)\, \mathrm{d}t \tag{13}$$

with an appropriate initial condition. Since the energy is conserved in eq 8, $H(\sigma)$ in eq 13 is actually a constant along a path. Thus, combining eqs 11−13, we see

$$-\frac{\partial S_{HJ}}{\partial t} = \frac{1}{2}\sum_k \left(\frac{\partial S_{HJ}}{\partial q_k}\right)^2 + V(q) \tag{14}$$

In the starting equation, eq 4, one must assign the parities to the individual coordinates. This procedure may require a coordinate transformation in q-space. Specifying the parity set implies that the entire space is divided into two parts as seen in eq 10, with one having real-valued momenta (positive parities) and the others bearing pure imaginary momenta (negative parities), although energy exchange among these two subspaces takes place (the total energy is conserved). As long as the parity set is kept fixed, so is the separation of the space. Thus, different type of solutions are given by resuming at eq 4 with a different set of parities and different directions associated with the negative parities. The global tunneling solution should be described in terms of path integration over many of those different paths and connecting the paths of different parity sets.

2. Tunneling Probability. A local semiclassical wave function is given as

$$\psi = A \exp\left(\frac{i}{\hbar} S_{HJ}\right) \tag{15}$$

where the preexponential factor A represents the amplitude. Since the HJ action, S_{HJ} in eq 13, is generally complex-valued, we rewrite S_{HJ} in the standard form as

$$S_{HJ} = S_R + iS_I \tag{16}$$

Inserting eq 16 into eq 15, we see

$$\psi = A \exp\left(-\frac{1}{\hbar}\left|S_I\right|\right) \exp\left(\frac{i}{\hbar} S_R\right) \tag{17}$$

where the phase convention to S_{HJ} is taken so that S_I becomes positive. From eq 17, dumping of the norm due to tunneling is estimated as

$$\exp\left(-2\,\frac{|\mathrm{Im}\, S_{HJ}|}{\hbar}\right) \tag{18}$$

It is generally expected that the magnitude of the imaginary part should become larger as more negative parities are used, which results in an exponentially smaller tunneling probability. Therefore, we henceforth consider only tunneling paths with one negative parity.

In applying the tunneling paths in a semiclassical method, particular quantum phases such as the Maslov phase arise at the entrance and exit points of a tunneling path. The reader should refer to refs 14−19 for this aspect. However, we simplify the calculation here by neglecting the semiclassical amplitude and all the quantum mechanical phases. Only the distribution of paths in configuration space, in which the tunneling contribution is included, is utilized to simulate the density of a wave packet. We call this simplified approach the time-dependent quasi-semiclassical trajectory (TDQSCT) method.

3. Branching of the Trajectories and Survival Probabilities. To estimate the tunneling probability, it is crucial to recognize that each path can bifurcate many times because of tunneling. Those paths that are born from tunneling can further branch. Another characteristic feature to the quasi-semiclassical approach is that a weight (mimicking the quantum population $|A|$ arising from A of eq 17) is assigned to each path. The weight of a path is unity at $t = 0$ and can change every time the branching occurs. Let us consider a single incidence of tunneling bifurcation of a trajectory. Assume that the weight of this trajectory happens to be P before this tunneling. Here, a tunneling path emanates from it, and this classical path keeps running even after this event. Then, there are three patterns in tunneling paths (see a schematic example in Figure 1).

(A) Path of direct tunneling, which simply travels through the tunneling space into the neighboring basin, thereby accomplishing the tunneling (Figure 1A). The associated tunneling probability is given by $p = P \exp(-2|\mathrm{Im}\, S_{HJ}|/\hbar)$, where S_{HJ} is the relevant action integral. On the other hand, the classical trajectory keeps running with a remaining weight $s\nu(t) = P[1 - \exp(-2|\mathrm{Im}\, S_{HJ}|/\hbar)]$. In this particular study, those paths achieving tunneling are forced to quit after the tunneling.

(B) Tunneling path of fading away deep into the tunneling space and not coming back to the classical space (Figure 1B). This path does not contribute to the tunneling at all, since $P \exp(-2|\mathrm{Im}\, S_{HJ}|/\hbar) = 0$, and the classical trajectory runs as though nothing happened, retaining the same weight P.

(C) Tunneling path that comes back to the classical space in the original basin, where a new classical trajectory is "born" (Figure1C). We now have two classical trajectories: the mother trajectory with a weight $s\nu(t) = P[1 - \exp(-2|\mathrm{Im}\, S_{HJ}|/\hbar)]$ and the daughter classical trajectory having the weight $s\nu(t) = P \exp(-2|\mathrm{Im}\, S_{HJ}|/\hbar)$. The sum of the weights of these two classical trajectories is invariant, and since both trajectories remain in the original potential basin, they do not contribute to acquiring the tunneling probability at this instance. However, these trajectories can further bifurcate and generate tunneling paths afterward.

4. Tunneling Points. We locate next the tunneling points from which a tunneling path can branch. Suppose a classical trajectory starts at a phase space point $(q(0), p(0))$ and reaches $(q(t), p(t))$ in time t. Taking into account the fact that both $q(0)$ and $p(0)$ are independent variables, one can define the density of trajectories at a point $q(t)$ in such a way that

$$\frac{\partial p(t)}{\partial q(t)} \equiv \det\left(\left[\frac{\partial p(t)}{\partial q(0)}\right]\left[\frac{\partial q(0)}{\partial q(t)}\right] + \left[\frac{\partial p(t)}{\partial p(0)}\right]\left[\frac{\partial p(0)}{\partial q(t)}\right]\right) \tag{19}$$

where, for instance, $[\partial p(t)/\partial q(0)]$ is a Jacobian matrix. The physical meaning of this expression is as follows: A small deviation of the initial position $q(0) \rightarrow q(0) + \Delta q$ would shift the final position as $(q(t), p(t)) \rightarrow (q(t) + \delta q, p(t) + \delta p)$. Then, $\delta p/\delta q$ represents the concentration of the trajectories projected onto the configuration space at $q(t)$, the trajectories which were initially included in the interval of Δq. The same thought applies

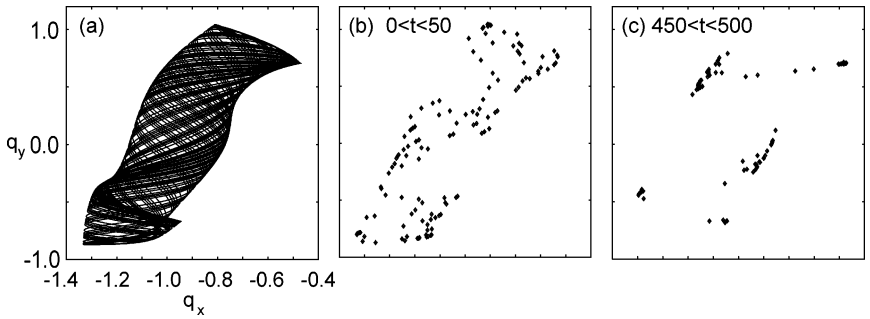

Figure 2. Time evolution of the tunneling points. (a) A classical trajectory trapped inside the left basin. (b) Tunneling points generated on this trajectory during $0 < t < 50$. (c) Those for $450 < t < 500$. As time passes, the tunneling points tend to be shifted to the envelope line of the path in panel (a) and seem more like the so-called turning points.

independently to an initial shift in momentum space such that $p(0) \rightarrow p(0) + \Delta p$. We should sum these two independent contributions after taking a limit of $\Delta q \rightarrow 0$ and $\Delta p \rightarrow 0$. Equation 19 describes these treatments collectively in multidimensional phase space. Incidentally, $|\partial p(0)/\partial q(t)|$ and $|\partial q(0)/\partial q(t)|$ appear as the amplitude factors of the semiclassical kernels $K(q, q_0, t)$ and $K(q, p_0, t)$, respectively. The caustic points at which $\partial p(0)/\partial q(t) = \infty$ ($\partial q(0)/\partial q(t) = \infty$) bring about a divergence to $K(q, q_0, t)$ ($K(q, p_0, t)$). Since we are seeking the places of high density of the trajectories in q-space, it is natural to take account of the caustics both of $K(q, q_0, t)$ and $K(q, p_0, t)$ systematically. On the basis of this geometrical characteristic, we define the tunneling points to be those that make $\partial p(t)/\partial q(t)$ infinity. For more details, see ref 14.

For a tunneling path to branch from its mother trajectory, two more conditions are required: a smooth connection between these paths and the initial direction (momentum) of the tunneling path. We refer these rather precise aspects to ref 14.

An important fact to be noted in our study is that the tunneling points are not fixed in space−time but are evolved, in clear contrast to the so-called turning point in the energy domain dynamics. For instance, the turning points for a one-dimensional oscillator are those satisfying $E = V(q)$. However, not only the number, but also the location, of the tunneling points can change in time, as shown in Figure 2.

C. Initial Conditions for Sampled Paths in Quasi-Semiclassical and "Classical" Calculations. We determine the initial conditions of sampled trajectories in phase space in terms of the Wigner distribution function[23]

$$\Gamma_{QM}(q, p) = \left(\frac{1}{2\pi\hbar}\right)^N \int \mathrm{d}x \Phi^*\left(q + \frac{x}{2}\right)\Phi\left(q - \frac{x}{2}\right) \exp\left[\frac{i}{\hbar} px\right] \tag{20}$$

For a coherent Gaussian function like eq 2, $\Gamma_{QM}(q, p)$ happens to be equal to the direct product of $|\Phi(q)|^2$ and $|\tilde{\Phi}(p)|^2$, where $\tilde{\Phi}$ is the momentum representation of Φ. Although other phase-space distribution functions (for instance, see refs 24 and 25) may be applied, we adopt this product for this particular purpose. It is well-known that as the lowest order of the full quantum equation of motion in phase space, the classical Louiville equation, is obtained as

$$\left[\frac{\partial}{\partial t} + \frac{\partial H}{\partial p}\frac{\partial}{\partial q} - \frac{\partial H}{\partial q}\frac{\partial}{\partial p}\right]\Gamma_{CL}(q, p, t) = 0 \tag{21}$$

where $\Gamma_{CL}(q, p)$ is accordingly the lowest approximation to the exact $\Gamma_{QM}(q, p)$ and is usually regarded as one of the semiclassical approximations.[26,27] We put the subscript CL on $\Gamma_{CL}(q, p)$ in this particular study to stress that no tunneling path is taken into account. Thus, $\Gamma_{CL}(q, p)$ can be propagated only with classical trajectories. The difference

$$\Gamma_{QM}(q, p, t) - \Gamma_{CL}(q, p, t) \tag{22}$$

and all the quantities associated with this difference represent the intrinsic quantum effect originated from the nonclassical dynamics.

From the semiclassical point of view, the tunneling seems to be achieved through two channels. Recall first that $\Gamma_{CL}(q, p, 0)$ made from the wave packet Φ having $E_{center} = 0.06$, which is lower than the barrier height, has components whose classical energies are high enough to surmount the barrier. Thus, these classical trajectories may represent the decay within the scheme of classical dynamics. The tunneling thus represented is called shallow tunneling. On the other hand, the lower-energy component of $\Gamma_{QM}(q, p, t)$ can also leak from the basin because of quantum wave penetration into the potential barrier. This part of tunneling should be described only in the higher-order terms of the Wigner function, as in eq 22. This is called the deep tunneling, which indeed requires nonclassical paths. The so-called dynamical tunneling is another well-known example, which is tunneling between two disjointed classical tori in phase space. The paths in the generalized classical mechanics that are considered in the preceding subsections are intended to represent paths of the deep tunneling. The inevitable coexistence of deep and shallow tunnelings constitutes a generic situation when tunneling dynamics is studied with a quantum wave packet. In the present study, our focus is placed on the effect of the deep tunneling, and therefore, all the quantities arising from $\Gamma_{CL}(q, p, t)$ alone are referred to as classical ones in what follows.

There are basically two ways of sampling the classical paths based on $\Gamma(q, p, 0)$ (no matter whether the tunneling paths are to be bifurcated eventually): (i) a uniform random sampling from a uniform phase space, and to each path, the value $\Gamma(q, p, 0)$ is assigned; and (ii) the so-called importance sampling to mimic the distribution $\Gamma(q, p, 0)$, but all the paths are initially (only initially) associated with unity as the value of the existing probability. The second procedure is not always possible, in general, since the Wigner distribution can locally take a negative value in general. However, as far as the our chosen initial wave function, namely, the coherent Gaussian is concerned, $\Gamma(q, p, 0)$ is positive semidefinite everywhere. For simplicity of the calculations, we take the second approach in this paper.

D. Survival Probability. Quantum mechanical survival probability against the leak of a wave packet in the region Ω is defined as[28]

$$SP_{QM}(t) = \int_\Omega \Phi(q, t)^* \Phi(q, t)\, \mathrm{d}q \tag{23}$$

According to the quasi-classical method, the corresponding

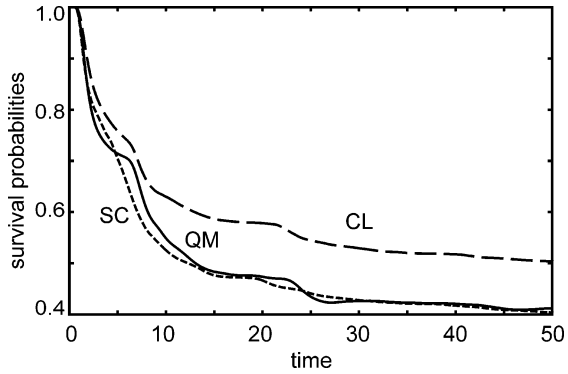

Figure 3. Quantum (QM, full line), quasi-semiclassical (SC, dotted line), and classical (CL, dashed line) survival probabilities.

classical survival probability is given as

$$\mathrm{SP}_{\mathrm{CL}}(t) = \frac{\sum_{q\in\Omega} M(q, t)}{M} \tag{24}$$

where M is the total number of sampling paths, and $M(q, t)$ is the number of classical paths found in a small bin at q in Ω and at time t. To calculate the quasi-semiclassical survival probability, it should be taken into account that a single trajectory can undergo the three types of branching many times, changing its weight P anew in a recursive manner as discussed in section II.B.3. The survival probability is thus given as the ratio of the sum of all the weights $s\upsilon_i(t)$ counted over the trajectories i that remain in the original basin to the total initial weights (M), that is, the total number of the initial trajectories. (See section II.B.3. for $s\upsilon(t)$.) We thus have

$$\mathrm{SP}_{\mathrm{SC}}(t) = \frac{\sum_{i=1}^{M} s\upsilon_i(\mathrm{t})}{M} \tag{25}$$

III. Characteristics of Tunneling in Early and Late Stages

A. Total Profile of the Survival Probability. For the system described in section II.A., the survival probabilities obtained by quantum (QM), quasi-semiclassical (SC), and classical (CL) methods are shown in Figure 3 as a function of time. The classical and quasi-semiclassical survival probabilities were estimated with 1000 trajectories. The so-called local analytic integrator (LAI) was used for integration of trajectories.[29] As seen in the figure, the global decay process is superposed with a steplike feature in any level of approximation. This stepwise feature arises from the swinging motion of the wave packet or the ensemble of classical trajectories in the basin: When the packet happens to be located at the remote site from the potential barrier, the decay slows down. It is also interesting to realize that the classical decay lasts long even after the major bunch of trajectories have escaped. This is because the coupling among different modes keeps causing the dispersion or randomization of energy among them, and the remaining trajectories can eventually acquire an energy in the mode of crossing over the barrier.

B. Fast Tunneling in the Early Stage and Slow Tunneling in the Late Stage. To identify the (deep) tunneling contribution alone, we subtract the classical survival probability from the full quantum counterpart, defining

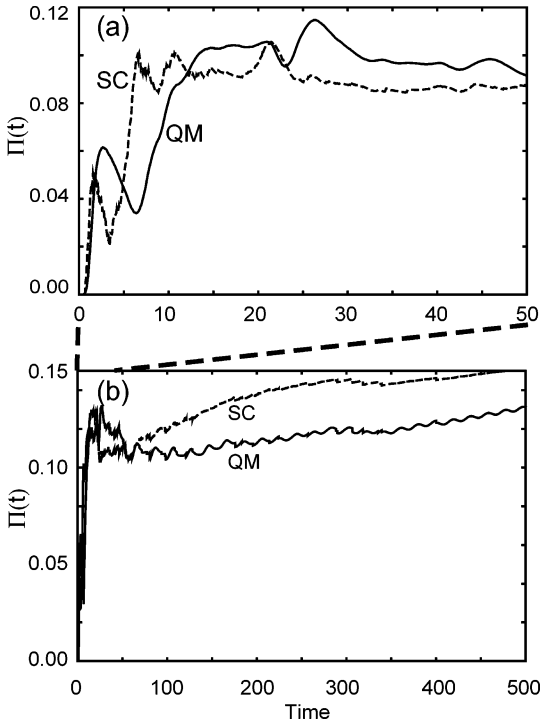

Figure 4. Difference between the classical and quantum survival probabilities (full line) denoted by QM. The same between the classical and quasi-semiclassical survival probabilities (dotted line) is denoted by SC. Panel (a) is a magnification of panel (b).

$$\Pi_{\mathrm{QM}}(t) = [1 - \mathrm{SP}_{\mathrm{QM}}(t)] - [1 - \mathrm{SP}_{\mathrm{CL}}(t)] \tag{26}$$

where $1 - \mathrm{SP}_{\mathrm{QM}}(t)$ and $1 - \mathrm{SP}_{\mathrm{CL}}(t)$ are, respectively, the quantum and classical populations that have leaked away from the basin accumulated by time t. We also define $\Pi_{\mathrm{SC}}(t)$ in a similar way. Basically, $\Pi_{\mathrm{QM}}(t)$ represents the total population that leaks from the basin up to time t because of quantum effects in the sense of eq 22. Figure 4b shows $\Pi_{\mathrm{QM}}(t)$ and $\Pi_{\mathrm{SC}}(t)$ in somewhat long-scale dynamics for $0 < t < 500$, whereas panel (a) magnifies the part of the early-stage dynamics $0 < t < 50$. Panel (a) strongly suggests that the massive tunneling leak has taken place in the very early stage of the dynamics; the majority of tunneling is accomplished by the time of $t \approx 15$, and after it, the tunneling rate becomes very small. Since the quasi-semiclassical survival probability shows a good agreement with the full quantum value, it supports the view that the tunneling is dominated by the early-stage dynamics.

In Figure 4a is observed a fine structure for $\Pi_{\mathrm{QM}}(t)$; it increases quickly to have a peak at about $t = 3$ but soon dumps, making a bottom at about $t = 7$. This implies that the classical decay should have a retardation relative to the quantum counterpart, or the first massive quantum leak takes place in advance of the classical one. One may wonder however that this time lag may strongly depend on the fact that we have chosen the Wigner distribution as an initial condition. However, a similar feature is observed in the quasi-semiclassical quantity $\Pi_{\mathrm{SC}}(t)$ (Figure 4), for which the initial condition of the classical paths $\Gamma(q, p, 0)$ is completely the same as that for the classical simulation. Therefore, the time lag in the early stage of the decay should be a reflection of the tunnel effect.

After $t = 100$, both $\Pi_{\mathrm{QM}}(t)$ and $\Pi_{\mathrm{SC}}(t)$ become much more steady. This type of tunneling in the late stage is called "slow tunneling" in this paper. Since the slow tunneling lasts for a very long time, it is conceived to dominate the static quantities

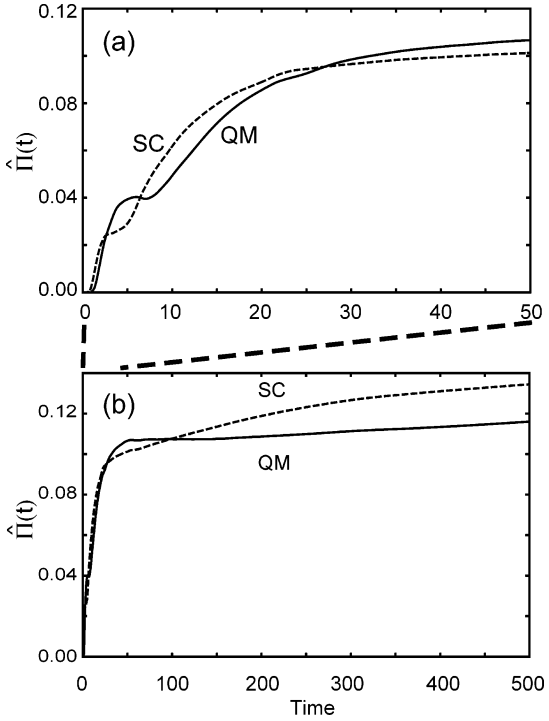

Figure 5. Accumulated tunneling probabilities averaged over the time *t*. See eq 28. Panel (a) is a magnification of panel (b). QM and SC denote quantum and quasi-semiclassical results, respectively.

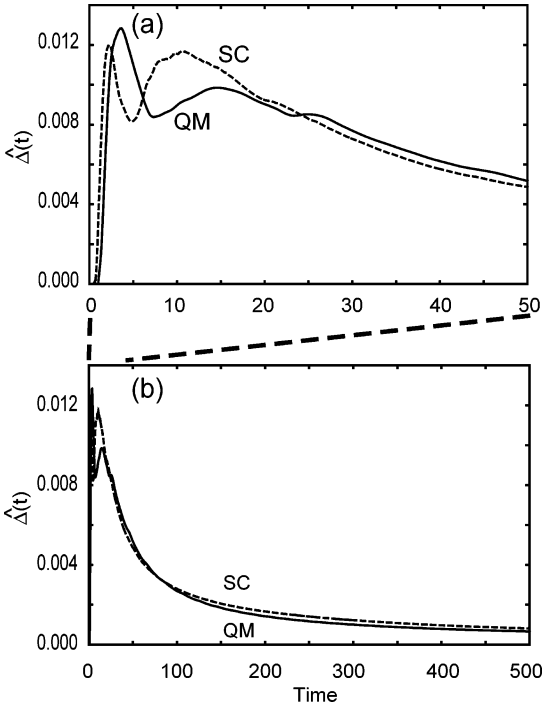

Figure 6. Tunneling rate with respect to the unit population that remains in the basin at time *t*. The data are averaged in the maner of eq 30. Panel (a) is a magnification of (b). QM and SC denote quantum and quasi-semiclassical results, respectively.

to be observed in the energy domain such as the tunnel splitting. Furthermore, $\Pi_{QM}(t)$ increases almost linearly, the slope of which seems to give an estimate of the tunneling rate. To be more precise, however, the time-dependent tunneling rate should be defined as

$$\frac{1}{SP_{QM}(t)}\frac{d\Pi_{QM}(t)}{dt} \tag{27}$$

However, the numerically given curves of $\Pi_{QM}(t)$ and $\Pi_{SC}(t)$ are too rugged to take a derivative, and hence, we smooth them by averaging as

$$\hat{\Pi}_{QM}(t) = \frac{1}{t}\int_0^t \Pi_{QM}(s)\, ds \tag{28}$$

Likewise $\hat{\Pi}_{SC}(t)$ is defined. As is shown in Figure 5, the overall features of both $\hat{\Pi}_{QM}(t)$ and $\hat{\Pi}_{SC}(t)$ now appear to be monotonically increasing, although the effect of the time lag of the classical decay is still noticeable. The smoothed curves also suggest that the tunneling rate becomes slow as time passes. To quantify this visual impression, we consider the tunneling rate for a given population remaining in the basin at time *t*, which is defined as

$$\Delta_{QM}(t) = \frac{1}{SP_{QM}(t)}\frac{\hat{\Pi}_{QM}(t+\Delta t) - \hat{\Pi}_{QM}(t)}{\Delta t} \tag{29}$$

where Δt is a short time interval. $\Delta_{QM}(t)$ is also oscillatory when a very small limit of Δt is taken. Therefore, once again, we smooth it by taking its average as

$$\hat{\Delta}_{QM}(t) = \frac{1}{t}\int_0^t \Delta_{QM}(s)\, ds \tag{30}$$

Figure 6 displays the global feature of $\hat{\Delta}_{QM}(t)$ (panel (b)) and its magnification for the early stage (panel (a)). It shows explicitly that the tunneling rate becomes smaller as time passes. (Recall that this is not the total amount of the tunneling population at time *t*.) With the above time average, the $\hat{\Delta}_{QM}(t)$ seems to be approaching an asymptotic value very slowly. In reality, the decay part of Figure 6b turns out to be of a form of the power of *t*, that is $t^{-\alpha}$ (with α being a little smaller than unity), which indicates that the tunneling decay rate (per unit population) is scale-invariant with respect to time *t* and does not seem to converge to a constant as far as this time range is concerned. Besides, this numerical result suggests that

$$SP_{QM}(t) = SP_{QM}(0)\exp(-ct^{1-\alpha}) + \text{rest}(t) \tag{31}$$

where the first term on the right-hand side represents decay due to tunneling alone and the second one does the rest. This is valid only when the tunneling decay is physically independent from all the other mechanisms that cause decay. However, the general validity of eq 31 and the associated mechanism are yet uncertain. In any case, we have thus confirmed that the rate of the tunnel decay is very fast in the initial stage, the reason for which is analyzed below.

C. Origin of the Fast Tunneling in the Early Stage. Judging from the good agreement of our quasi-semiclassical survival probability with the full quantum values, we think we may utilize this method for an analysis of the origin of the fast tunneling in the early stage. We recall in Figure 4 that the first massive tunneling took place around $t = 3$. To understand this, we first note that the tunneling points are time-dependent and generated as a result of nonlinear dynamics, since the quantities in eq 19 are all determined through an equation of motion for the stability matrix.[29] In other words, the tunneling points evolve in time in clear contrast to the so-called turning points considered in the stationary-state (energy domain) semiclassical mechanics.

We first show the time dependence of the number of tunneling points during $0 < t < 20$ (Figure 7). It turns out that the time dependence is rather strong. In particular, we observe a

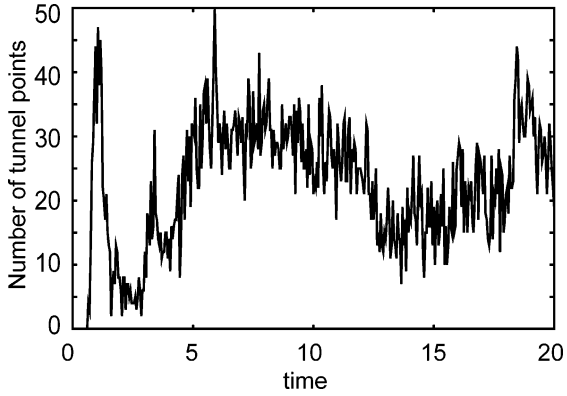

Figure 7. Fluctuation of the number of the tunneling points in time in the early stage.

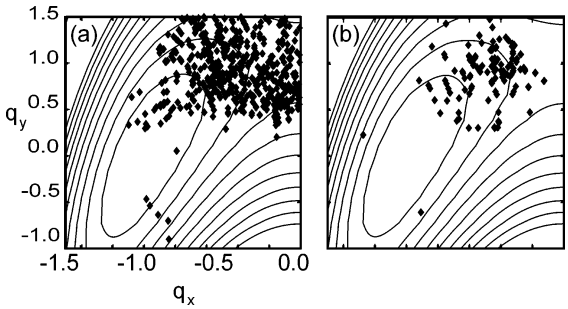

Figure 8. Spatial distribution of the tunneling points generated during (a) $0 < t < 10$ and (b) $400 < t < 410$.

significant fluctuation before $t \approx 5$ and a sharp peak at $t = 2$. Thus, it is conceived that the tunneling paths that were generated at $t \approx 2$ should have taken much population out of the basin and spend a short time $t \approx 1$ to reach the absorbing boundary. Thus, this collective event should have caused the rapid decay of the survival probability at this very early stage around $t = 3$. After this, the distribution of the tunneling points seems to be dispersed, and time dependence of the fluctuation become rather steady. However, it is also clear from Figure 7 that the number of the tunneling points alone does not account for the entire behavior in Figure 6.

We therefore examine the spatial distribution of the tunneling points that are generated during a given time interval at two selected times (Figure 8); one is sampled in the early stage $0 < t < 10$ (panel (a)), and the other is taken from a later stage $400 < t < 410$ (panel (b)). Above all, it is noticed in Figure 8 that the number of the tunneling points yielded during $0 < t < 10$ is much larger than that observed in the period of $400 < t < 410$. This is merely a reproduction of the above fact. Another important fact is that the tunneling points in the early stage have a much wider distribution in space. In particular, there are many tunneling points deep in the transition-state region. Obviously, these tunneling points have been marked by the trajectories of high energy, and the resultant tunneling paths are supposed to have equally high energies due to the energy conservation.[15] Hence, the tunneling paths of high energy tend to readily escape because of the geometrically favorable location of the tunneling points. In addition, the geometrical length of these tunneling paths should be short, since they will soon reach the next basin. Furthermore, given a high energy and a short pathway, a tunneling path should have small |Im S_{HJ}| (see eq 18), which implies that the associated tunneling probability is expected to be generally high.

The role of classical trajectories having energy higher than the potential barrier is particularly interesting. Even if the total energies are higher than the barrier, some of them do not surmount the barrier at once and return to the basin area, if the energy is concentrated in the mode transversal to the reaction coordinate. This can happen only in the multidimensional system. These trajectories can give birth to tunneling paths before they finally accomplish their own classical escape. This tunneling is regarded as dynamical tunneling by definition.[30,31] Therefore, the mother classical trajectories should lose their survival probability $s\nu(t)$, compensating the population of the newly born tunneling paths. Since even these remaining classical trajectories eventually escape from the basin classically,[32] the overall escape probability accumulated (time-integrated) from all these classical trajectories and associated tunneling paths should be unchanged by the presence of the dynamical tunneling. However, the time profile of the decay may be strongly affected, since the escape in the early stage is greatly enhanced (accelerated) by the dynamical tunneling. It is quite likely that the first massive quantum leak at about $t = 3$ occurring ahead of the classical one (Figure 4a) is partly due to these tunnelings above the potential barrier.

All these characteristic events happen in the early stage, since the classical paths of such high energies disappear from the basin in some relatively short time, as the classical survival probability $SP_{CL}(t)$ shows in Figure 3. As a result, only the classical paths of low energy remain in the basin without classical escaping, which give birth to the tunneling points only in the deep region of the basin. For exactly the opposite reason to the case of the high-energy paths, tunneling paths branched from such low-energy classical paths tend to have a small tunneling probability. Hence, tunneling in the late stage is not as active as in the early stage. It is concluded therefore that the space−time evolution of the tunneling points causes the fast tunneling in the early stage and a slow feature in the late stage.

Another interesting feature observed in Figures 4 and 5 is that $\Pi_{SC}(t)$ ($\hat{\Pi}_{SC}(t)$) becomes a little larger than $\Pi_{QM}(t)$ ($\hat{\Pi}_{QM}(t)$) in the later stage. Since

$$\Pi_{SC}(t) - \Pi_{QM}(t) = SP_{QM}(t) - SP_{SC}(t) \tag{32}$$

this implies that the full quantum mechanical survival probability is larger than the quasi-semiclassical counterpart. This is presumably explained in terms of the role of periodic orbits,[1] but this aspect is beyond the scope of the present paper.

D. Isotope Effect in the Time Domain. We finally explore the dynamical isotope effect that may be observed experimentally in the time domain. The quantum mechanical survival probability of a proton is compared with that of a deuteron on the same potential function as above. For the corresponding deuteron transfer system, we set the mass $m = 2$, assuming that the other part of a molecule supporting the deuteron is very heavy. Figure 9 shows the difference between the quantum survival probability of a proton and that of a deuteron, that is

$$\Pi_{DP} = SP_{QM,deuteron} - SP_{QM,proton} \tag{33}$$

The tunneling rate of the deuteron should be much smaller. Hence, Π_{DP} is always positive as seen in Figure 9. Besides the tunneling, the dynamics of the deuteron should bear more classical nature in any aspect. In this aspect, it should make sense to compare $\Pi_{DP}(t)$ with $\Pi_{QM}(t)$ in eq 26, since

$$\Pi_{QM}(t) = SP_{CL,proton} - SP_{QM,proton} \tag{34}$$

The overall features of $\Pi_{DP}(t)$ with $\Pi_{QM}(t)$ are somewhat

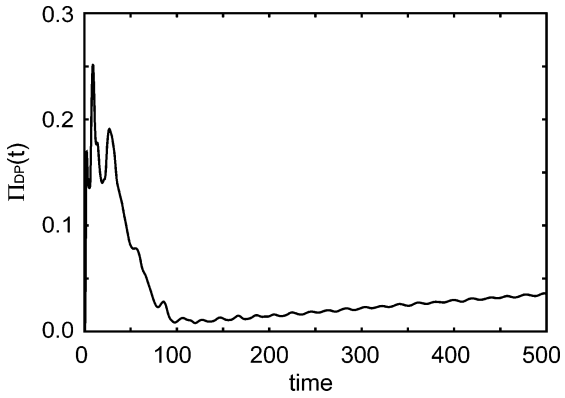

Figure 9. Difference of the quantum survival probabilities for deuteron and proton; $SP_{QM,deuteron} - SP_{QM,proton}$.

similar, although this comparison is not necessarily a consistent one, since $\Pi_{QM}(t)$ includes $SP_{CL,proton}$ rather than $SP_{CL,deuteron}$.

Returning to Figure 9, we emphasize that Π_{DP} is also strongly time-dependent. In the early stage of the reaction, $t < 100$, the difference is very large and oscillatory, reflecting the complicated dynamics arising from not only tunneling but also the difference in the speed of wave packet motions. This fact also suggests that tunnel effect is important especially in the early-stage dynamics. $\Pi_{DP}(t)$ becomes very small at about $t = 100$, which implies that the massive escape of the deuteron wave packet is also accomplished by this time. After $t = 100$, it increases very slowly for a long time ($t > 100$). Again, this almost linear increase should reflect a difference between the tunneling rates of a proton and a deuteron. The present example demonstrates that both "fast" and "slow" tunneling can be observed in a real time measurement.

Concluding Remarks

We have discussed the time-dependent characteristics of quantum mechanical tunneling: fast tunneling in the early stage and slow and long-lasting tunneling in the later stage. They have been studied from two aspects; one is time-dependent quasi-semiclassical theory to understand the physical origin of the characteristics, and the other is a possible experimental realization of it through an isotope effect.

Using the quasi-semiclassical theory, we have clarified the relationship between survival probability and the tunneling points; the space−time evolution of the tunneling points is primarily important to describe the difference of the tunneling dynamics in the early and late stages. In particular, we have discussed the role of dynamical tunneling to characterize the time dependence of tunneling dynamics that is not appreciated in the integrated survival probability. Slow tunneling in the long time region is also important, because it should dominate the time-independent feature of tunneling that should be observed through stationary quantities such as the tunneling splitting. Such characteristics of tunneling dynamics may be directly observed in terms of the isotope effect. So far, the experimental studies on tunneling are made mostly in the energy domain. However, by performing a pump−probe experiment of the excited-state proton transfer and monitoring the survival probability before and/or after the reaction on the excited state, and by comparing proton transfer with deuteron transfer, the time-dependent features of tunneling dynamics discussed in this paper should be observed in real time.

Acknowledgment. This work has been supported in part by a Grant-in-Aid for Basic Studies and the 21st Century COE Program for Frontier in Fundamental Chemistry from the Ministry of Education, Science, Culture, Sports, Science, and Technology of Japan. We are grateful to the support from JSPS for the Japan−Germany cooperative research project.

References and Notes

(1) Budiyono, A.; Takatsuka, K. Submitted for publication.
(2) Ushiyama, H.; Takatsuka, K. *Angew. Chem., Int. Ed.* **2005**, *44*, 1237.
(3) Giese, K.; Ushiyama, H.; Takatsuka, K.; Kühn, O. *J. Chem. Phys.* **2005**, *122*, 124307.
(4) Ushiyama, H.; Takatsuka, K. *J. Chem. Phys.* **2001**, *115*, 5903.
(5) Bountis, T., Ed. *Proton transfer in hydrogen-bonded systems*; Plenum Press: New York, 1992.
(6) Benderskii, V. A.; Makarov, D. E.; Wight, C. A. Chemical Dynamics at Low Temperatures. *Adv. Chem. Phys.* **1998**, *88*, 1.
(7) Zewail, A. H. *J. Phys. Chem. A* **2000**, *104*, 5660.
(8) Douhal, A.; Kim, S. K.; Zwail, A. H. *Nature (London)* **1995**, *378*, 260.
(9) Fiebig, T.; Chachisvilis, M.; Manger, M. M.; Zewail, A. H. *J. Phys. Chem. A* **1999**, *103*, 7419.
(10) Takeuchi, S.; Tahara, T. *J. Phys. Chem.* **1998**, *102*, 7740.
(11) Takeuchi, S.; Tahara, T. *Chem. Phys. Lett.* **1998**, *228*, 1.
(12) Takeuchi, S.; Tahara, T. *Chem. Phys. Lett.* **2001**, *347*, 108.
(13) Wilkinson, S. R.; Bharucha, C. F.; Fischer, M. C.; Madison, K. W.; Morrow, P. R.; Niu, Q.; Sundaram, B.; Raizen, M. G. *Nature (London)* **1997**, *387*, 575.
(14) Ushiyama, H.; Takatsuka, K. *J. Chem. Phys.* **2004**, *120*, 4561.
(15) Takatsuka, K.; Ushiyama, H. *Phys. Rev. A* **1995**, *51*, 4353.
(16) Ushiyama, H.; Takatsuka, K. *Phys. Rev. E* **1996**, *53*, 115.
(17) Ushiyama, H.; Takatsuka, K. *J. Chem. Phys.* **1997**, *106*, 7023.
(18) Ushiyama, H.; Takatsuka, K. *J. Chem. Phys.* **1998**, *109*, 9664.
(19) Takatsuka, K.; Ushiyama, H.; Inoue-Ushiyama, A. *Phys. Rep.* **1999**, *322*, 347.
(20) Kosloff, D.; Kosloff, R. *J. Comput. Phys.* **1983**, *52*, 35.
(21) Yoshida, H. *Phys. Lett. A* **1990**, *150*, 262.
(22) Takahashi, T.; Ikeda, K. *J. Chem. Phys.* **1993**, *99*, 8680.
(23) Wigner, E. P. *Phys. Rev.* **1932**, *40*, 749.
(24) Husimi, K. *Proc. Phys. Math. Soc. Jpn.* **1940**, *22*, 264.
(25) Takatsuka, K. *Phys. Rev. Lett.* **1988**, *61*, 504.
(26) Heller, E. J. *J. Chem. Phys.* **1976**, *65*, 1289.
(27) Heller, E. J. *J. Chem. Phys.* **1977**, *67*, 3339.
(28) In the literature, $|\int_\Omega \Phi(q, 0)^* \Phi(q, t)\, dq|^2$ is sometimes referred to as the survival probability, and $\int_\Omega \Phi(q, t)^* \Phi(q, t)\, dq$ is the nonescape probability. See, for example, Garcia-Calderon, G.; Mateos, J. L.; Moshinsky, M. *Phys. Rev. Lett.* **1995**, *74*, 337.
(29) Ushiyama, H.; Arasaki, Y.; Takatsuka, K. *Chem. Phys. Lett.* **2001**, *346*, 169.
(30) Davis, M. J.; Heller, E. J. *J. Chem. Phys.* **1981**, *75*, *246.*
(31) Hashimoto, N.; Takatsuka, K. *J. Chem. Phys.* **1998**, *108*, 1893. See Table 1 in this paper.
(32) We tentatively disregard the presence of periodic orbits and other exceptional trajectories having energy higher than the barrier yet do not surmount it.